atmosphere

MDPI

Review

The Impact of the Hunga Tonga–Hunga Ha'apai Volcanic Eruption on the Stratospheric Environment

Qian Sun [1], Taojun Lu [1], Dan Li [2,*] and Jingyuan Xu [2,3]

[1] Shenyang Aircraft Design and Research Institute, Aviation Industry Corporation of China, Shenyang 110035, China
[2] Key Laboratory of Middle Atmosphere and Global Environment Observation, Institute of Atmospheric Physics, Chinese Academy of Sciences, Beijing 100029, China
[3] College of Earth and Planetary Sciences, University of Chinese Academy of Sciences, Beijing 100049, China
* Correspondence: lidan@mail.iap.ac.cn

Abstract: In this study, an overview of two years of research findings concerning the 2022 Hunga Tonga–Hunga Ha'apai (HTHH) volcanic eruption in the stratospheric environment is provided, focusing on water vapor, aerosols, and ozone. Additionally, the potential impacts of these changes on aviation equipment materials are discussed. The HTHH volcanic eruption released a large amount of particles (e.g., ash and ice) and gases (e.g., H_2O, SO_2, and HCl), significantly affecting the redistribution of stratospheric water vapor and aerosols. Stratospheric water vapor increased by approximately 140–150 Tg (8–10%), with a concentration peak observed in the height range of 22.2–27 km (38–17 hPa). Satellite measurements indicate that the HTHH volcano injected approximately 0.2–0.5 Tg of sulfur dioxide into the stratosphere, which was partially converted into sulfate aerosols. In-situ observations revealed that the volcanic aerosols exhibit hygroscopic characteristics, with particle sizes ranging from 0.22–0.42 μm under background conditions to 0.42–1.27 μm. The moist stratospheric conditions increased the aerosol surface area, inducing heterogeneous chlorine chemical reactions on the aerosol surface, resulting in stratospheric ozone depletion in the HTHH plume within one week. In addition, atmospheric disturbances and ionospheric disruptions triggered by volcanic eruptions may adversely affect aircraft and communication systems. Further research is required to understand the evolution of volcanic aerosols and the impact of volcanic activity on aviation equipment materials.

Keywords: HTHH volcano; stratospheric water vapor; stratospheric ozone; stratospheric aerosol

Citation: Sun, Q.; Lu, T.; Li, D.; Xu, J. The Impact of the Hunga Tonga–Hunga Ha'apai Volcanic Eruption on the Stratospheric Environment. *Atmosphere* **2024**, *15*, 483. https://doi.org/10.3390/atmos15040483

Received: 23 January 2024
Revised: 8 April 2024
Accepted: 11 April 2024
Published: 13 April 2024

1. Introduction

On 15 January 2022, at approximately 4:10 AM UTC, the underwater volcano known as Hunga Tonga–Hunga Ha'apai (HTHH), located in the South Pacific islands (20.54° S, 175.38° W), erupted explosively. This event, marked by a Volcanic Explosivity Index (VEI) of 5 to 6, propelled an eruption plume to the mesosphere with a maximum altitude of ~57.5 km [1–3]. The volcanic eruption released a large amount of plume containing volcanic ash, ice clouds, and gases, including sulfur dioxide (SO_2), hydrogen chloride (HCl), and water vapor. These substances were injected into the stratosphere, triggering large disturbances to stratospheric water vapor and aerosols. Although only a small fraction of the volcanic plume reached the lower mesosphere, this eruption was the most powerful and remarkable volcanic activity in the last 30 years. According to measurements from geostationary satellites, the height of the volcanic plume reaching the mesosphere was the highest recorded height in recent years [2,4].

Despite the intense eruptive activity of the HTHH volcano, satellite observations indicate that the total amount of sulfur dioxide (SO_2) released by this eruption was initially only 0.2 to 0.5 Tg [3,5,6]. This value is significantly lower than the 14 to 23 Tg of SO_2 released by the Pinatubo volcano in 1991 [7]. Preliminary estimations based on existing

stratospheric chemistry theories, observational data, and climate models, suggest that the volcanic eruption of HTHH will not greatly impact the global climate. Within 1 to 2 years after the volcanic eruption, the surface temperature decreased by only 0.01 °C to 0.1118 °C [8,9]. However, recent research results indicate that, 17 months after the eruption, stratospheric aerosols from the HTHH volcano did not rapidly settle as initially expected. Instead, they only slightly settled and continued to persist in the stratosphere [10,11]. Moreover, the substantial injection of water vapor during the initial phase of the volcanic eruption accelerated chemical reactions leading to stratospheric ozone depletion [12]. Water vapor persisting in the stratosphere dominates the net warming effect at the top of the atmosphere [13], increasing the global mean surface temperature by 1.5 °C [14].

The increase in water vapor and sulfate aerosols in the stratosphere not only leads to ozone depletion [15], but also exerts far-reaching effects on other stratospheric chemical processes and the radiation balance. Furthermore, it plays a key role in contributing to global climate change. These changes potentially impact the materials used in aviation equipment. Therefore, it is essential to identify the evolution of ozone, water vapor, and aerosols in the stratosphere after the HTHH volcanic eruption. This overview includes three sections: the introduction, the impact of the HTHH volcano on the stratospheric environment (e.g., water, aerosol, and ozone), and, lastly, the discussion and conclusion section.

2. The Impact of the HTHH Volcanic Eruption on the Stratospheric Environment

2.1. The Impact of the HTHH Volcano on Stratospheric Water Vapor

Nineteen hours after the HTHH volcanic eruption, weather balloons carrying Vaisala RS41 radiosondes were launched in Nadi, Fiji (17.77° S, 177.45° E). The abnormal water vapor signals within the volcanic plume were detected in the measured profiles, with high vertical resolution [16]. The observational data revealed significantly elevated water vapor mixing ratios in the stratosphere, reaching up to 1300 ppmv at altitudes of 19–28 km, far exceeding the background water vapor value in the stratosphere (~5 ppmv). However, the balloon explosion occurred at 28 km, and no further information on the above water vapor profiles was obtained. Subsequently, weather balloons were launched at two sites on the east coast of Australia (Willis Island and Woodstock), and the maximum water vapor values reached 2900 ppmv, approximately 580 times greater than the background stratospheric water vapor (~5 ppmv). The COSMIC-2 satellite data validated these findings, showing that the water vapor value reached 2500 to 3500 ppmv at 29–33 km, which is consistent with the radiosonde measurements [17]. Water vapor injected into the stratosphere by the HTHH volcano diffuses globally with stratospheric circulation, and the maximum stratospheric water vapor at 19–28 km gradually weakens.

Conventional radiosondes cannot meet the precision requirements for measuring low stratospheric water vapor compared to abundant tropospheric water vapor. However, the Cryogenic Frostpoint Hygrometer (CFH) is an effective scientific instrument for detecting water vapor in the stratosphere. However, its high cost prevents it from being launched in the global operational upper air network. Twelve weeks after the eruption of the HTHH volcano, on 9 April 2022, the Institute of Atmospheric Physics of the Chinese Academy of Sciences launched radiosonde balloons from Lijiang, Yunnan (26.8° N, 100.2° E). The CFH measurements showed an enhanced water vapor signal at altitudes of 24–25 km in the extratropical westerly jet of the Northern Hemisphere (Figure 1: right). The measured water vapor value was 8 ppmv, and water vapor profiles from the Microwave Limb Sounder (MLS) also indicated an increase in water vapor at 20–30 hPa, with values of 6–7 ppmv [18,19].

Although radiosondes provide high vertical resolution profiles and detailed information on the vertical distribution of water vapor, their spatial and temporal coverage is limited. Therefore, sun-synchronous orbit satellite remote sensing data are crucial for studying the evolution of water vapor during the early stages of volcanic eruptions. Based on an analysis of Microwave Limb Sounder (MLS) satellite data, two high-level water vapor layers were observed in the stratosphere two days after the volcanic eruption (Figure 1: left). These layers consisted of a small amount of water vapor concentrated in the upper strato-

sphere at pressure heights of 1–8 hPa, and most of the water vapor was concentrated in the middle stratosphere at pressure heights of 10–80 hPa [3,6,19]. After 2 weeks, the slightly increasing water vapor in the upper stratosphere diffused rapidly, almost completely mixing with the surrounding background. Consequently, the disturbance to the background values decreased to a negligible level. In contrast, the diffusion rate of water vapor in the middle stratosphere was lower. During the first two weeks of the HTHH eruption, the height of the enhanced water vapor layer in the middle stratosphere slightly decreased, and then the positive anomalous water vapor extended throughout the tropics of the Southern Hemisphere within a few months (Figure 1: middle). Compared to zonal diffusion, the meridional diffusion of water vapor is slower and takes several months to diffuse to the Northern Hemisphere and even polar regions. The chemistry transport model (the Chemical Lagrangian Model of the Stratosphere, CLaMS) simulations indicated that within 1–2 months of the HTHH volcanic eruption, the deep branch of the Brewer–Dobson circulation and transport along isentropic surfaces shifted anomalously high levels of water vapor to the South Polar regions [3].

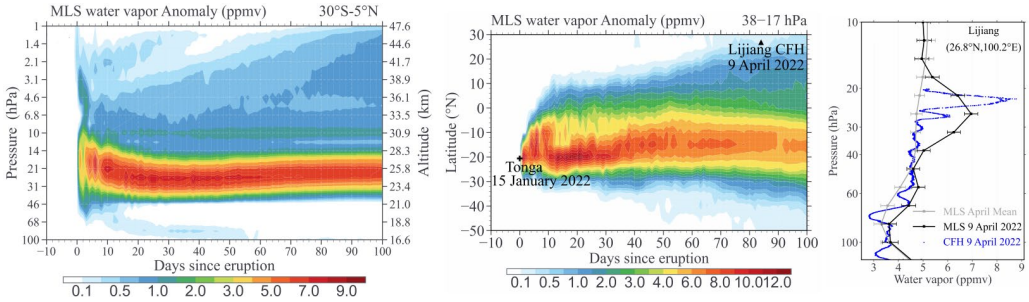

Figure 1. (**left**) MLS/Aura time series of mean (30° S–5° N) stratospheric water vapor anomalies (ppmv) from 100 to 1 hPa after the HTHH eruption (15 January 2022), from January–April 2022. The anomalies are calculated by subtracting the water vapor averaged 0–10 days prior to the eruption of the HTHH from the daily water vapor data. (**middle**) Zonal mean water vapor anomalies (ppmv) as a function of latitude and time at 38–17 hPa levels. The locations of the HTHH volcano and Lijiang are marked with a black plus symbol and a triangle, respectively. (**right**) Vertical profiles of water vapor at Lijiang on 9 April 2022, derived from in-situ observations (blue), and MLS remote sensing observations (black). The gray line shows the mean April water vapor with standard deviations derived from MLS during 2005–2020 (adapted from Xu et al., [19]).

In summary, the eruption of the HTHH volcano injected approximately 140–150 Tg of water vapor into the stratosphere [3,6,13,19], resulting in an increase of approximately 8–10% in stratospheric water vapor. The enhanced total amount of water vapor is different when using different versions of MLS data or balloon soundings. The anomalous amount of water vapor is approximately 50 Tg when using balloon measurements [16]. The enhanced value for water vapor is approximately 139 Tg when using MLS V4, and the 10-day mean value of water vapor before the volcanic eruption is selected as the reference value [19]. However, the positive anomaly value of water vapor is approximately 146 Tg when using the same version of MLS data, but the 2005–2021 January–February–March average value is selected as the background value [6]. The total amount of water vapor from the HTHH eruption was ~145 Tg when using the MLS V5 and selecting the 2021 data as the background value [13]. The enhanced water vapor was mainly concentrated in the altitude range of 22.2–27 km (38–17 hPa) in the Southern Hemisphere during the first year after the eruption. The substantial increase in water vapor led to a short-term infrared radiative cooling within this region, resulting in a temperature decrease of 4 K [20]. The cooling, in turn, triggered enhanced meridional winds at 20 hPa in the Southern Hemisphere [21]. Notably, stratospheric water vapor is an important greenhouse gas with a long lifetime and no significant sink in the stratosphere. Therefore, such a large injection of water vapor into the

stratosphere will persist for several years and will affect stratospheric chemistry, radiation balance, dynamic processes, and polar ozone depletion.

2.2. The Impact of the HTHH Volcano on Stratospheric Aerosols

High-spatio-temporal-resolution visible cloud images from the geostationary satellite Himawari-8 show the plume evolution of the HTHH volcanic eruption for one week. During the first eruption stage, the volcanic plume formed as a brownish-black mushroom-shaped cloud composed mainly of volcanic ash and water condensates (liquid water and ice crystals) [3,6]. However, two days after the eruption, the volcanic ash component was barely detectable in the ultraviolet imagery due to diffusion and gravitational settling effects [22]. Measurements from the Ozone Monitoring Instrument (OMI), the Tropospheric Monitoring Instrument (TROPOMI) and the Ozone Mapping and Profiling Suite (OMPS) onboard the European Space Agency's Sentinel-5P satellite, indicate that the HTHH eruption injected ~0.4–0.5 Tg of sulfur dioxide into the stratosphere [5]. Moreover, studies also indicate that the amount of SO_2 may reach 1.5 Tg due to the initial SO_2 being quickly converted into sulfates [23]. Two or three days after the volcanic eruption, sulfate aerosols were found to be the dominant component in the greenish plume observed by the Himawari-8 satellite [14]. This phenomenon is inconsistent with the typical rate of sulfate aerosol formation, which usually takes months for sulfur dioxide to oxidize and regenerate as sulfate aerosols under stratospheric temperature and humidity conditions. The rapid conversion of sulfur dioxide into sulfate aerosols could be attributed to the abundant presence of water vapor during the initial phase of the HTHH volcanic eruption [23–25]. After the volcanic eruption, French scientists conducted sounding measurements on Reunion Island in the Southern Hemisphere (La Réunion, 21.1° S, 55.3° E). Sounding balloons were launched with a portable Light Optical Aerosol Counter (LOAC) to detect volcanic aerosols [26]. Due to the stratospheric eastward wind belt in the Southern Hemisphere, Reunion Island was located downwind of the HTHH volcanic plume. The light optical aerosol counter showed an aerosol extinction coefficient up to ~4×10^{-3} km^{-1} at altitudes of 22.6 km and 24.9 km on 23 January. The observed aerosol extinction coefficient was 0.4×10^{-3} km^{-3} at 19.5 km on 26 January. In-situ measurements provide more quantitative information on volcanic plumes than satellite measurements do. The observed aerosol size distribution was unimodal, with aerosol radii smaller than 1 μm. This distribution is different from the bimodal distribution typically observed in volcanic aerosols [27]. According to the LOAC aerosol classification, aerosols with radii in the range of 0.5–1.0 μm appeared to be liquid or semitransparent, indicating that the volcanic plume mostly consisted of sulfate droplets. Particles with radii smaller than 0.5 μm were hygroscopic and semitransparent, suggesting that the dominant component of the aerosols was sulfate droplets enclosing volcanic ash, which is consistent with the results of Yuen et al. [28] regarding particle formation from magma–seawater interactions. Notably, satellite remote sensing measurements fail to retrieve relevant information regarding these small, absorptive aerosols [26].

To study the spatiotemporal distribution characteristics of atmospheric components over the Tibetan Plateau, the Atmospheric Composition sounding team from the Institute of Atmospheric Physics, Chinese Academy of Sciences, has conducted the Water Vapor, Ozone, and Particles (SWOP) campaign over the Tibetan Plateau since 2009 [29–32]. A Cryogenic Frost Point Hygrometer (CFH), a Compact Optical Backscatter Aerosol Detector (COBALD), and a Portable Optical Particle Spectrometer (POPS) were used to determine the particle size distribution, with diameters ranging from 0.13 to 3.0 μm. On 9 April 2022 (12 weeks after the HTHH volcanic eruption), balloon-borne measurements in Lijiang, Yunnan captured strong aerosol and water vapor signals at approximately 24–25 km in the westerly jet stream of the Northern Hemisphere (Figure 2). The COBALD and POPS observations provided the microphysical properties of volcanic aerosols, such as the backscatter ratio, particle concentration, and size distribution. The volcanic aerosol number density was approximately 1 cm^{-3} and mainly consisted of particles with diameters between 0.42 μm and 1.27 μm, which differed from the size distribution of stratospheric aerosols (without

the HTHH volcano), where the peak was between 0.22 μm and 0.42 μm [18]. The in-situ measurement data over the Tibetan Plateau characterize the features of the volcanic plume and will be useful for understanding the physical and chemical processes of the volcanic plumes.

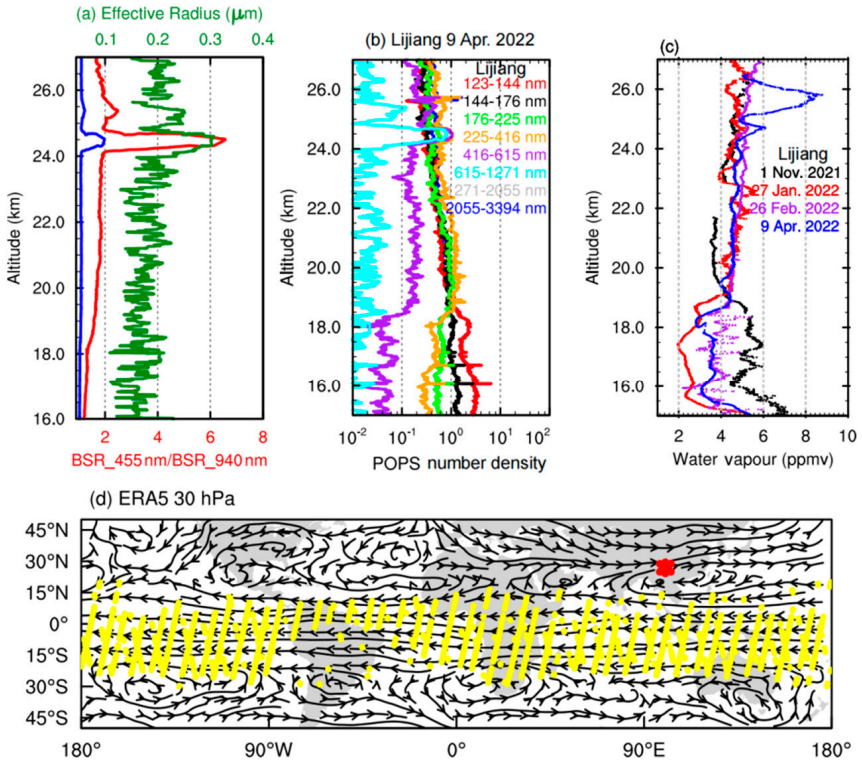

Figure 2. (**a**) Vertical profiles of the backscatter ratio (blue for 455 nm, red for 940 nm) data derived from the COBALD sonde and the effective radius (green) from the POPS measurements obtained in Lijiang on 9 April 2022. (**b**) Vertical profiles of the aerosol number density for bins of eight sizes from the POPS measurements obtained on 9 April 2022. (**c**) Profiles of water vapor on different days in Lijiang. (**d**) The European Centre for Medium-range Weather Forecasts (ECMWF) Reanalysis version 5 (ERA5) streamline data obtained at 30 hPa on 9 April 2022. The yellow dots mark the CALIPSO footprints when volcanic plumes (with altitudes of 22–25 km) were detected by an expedited level 2 vertical feature mask (VFM) algorithm on 7, 8, and 9 April. The asterisk marks the Lijiang site (from Figure 2 of Bian et al. [18]).

During the first three weeks after the volcanic eruption, the height of the volcanic plume decreased by several kilometers due to the net radiative cooling effect of water vapor (Figure 3). After several weeks, the gravitational settling of aerosols and the uplift of the water vapor layer caused the separation of the water vapor layer and the aerosol layer [3,23]. The phenomenon of aerosol and water vapor stratification has also been observed in volcanic plumes in the Northern Hemisphere [18]. Based on the preliminary understanding of volcanic eruptions and stratospheric chemistry, it is expected that the influence of stratospheric aerosol optical thickness will persist until mid-2023, with a total duration of 14 to 17 months for the volcanic eruptions. However, the latest satellite measurements confirm that there is almost no volcanic ash in the volcanic aerosol layer. The main component is sulfate aerosols (with an effective radius of ~0.4 μm). Despite the presence of the volcanic aerosol layer in the stratosphere for 17 months, there is only a slight reduction in particle size, and the estimated amount of sulfuric acid is 0.66 ± 0.1 Tg [10], which will continue to exist in the stratosphere and have a sustained impact on stratospheric chemistry, radiation, and dynamic processes.

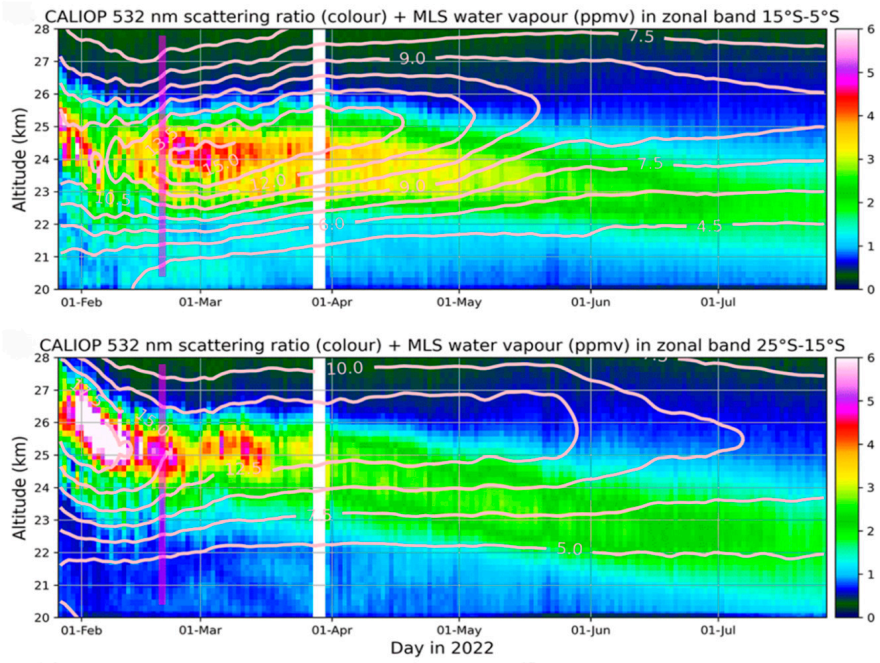

Figure 3. Panels (top, bottom) show zonal and latitude band averages as a function of time for the CALIOP 532 nm scattering ratio (color) and MLS water vapor (contours, ppmv) for the 15–5° S and 25–15° S latitude bands, respectively (adapted from Legras et al. [23]).

2.3. The Impact of the HTHH Volcano on Stratospheric Ozone

The eruption of the HTHH volcano injected a large amount of water vapor, along with a small amount of HCl, ClO, and other gases into the stratosphere. Radiosonde data and remote sensing observations indicate that the elevated water vapor layer induces radiative cooling and increases the surface area of stratospheric aerosols. This triggered heterogeneous chemical reactions of chlorine on the surface of volcanic aerosols in the plume soon after the HTHH eruption [33,34]. Under moist conditions on a volcanic aerosol surface, HCl is rapidly oxidized to ClO. In the presence of decreased NOx concentrations, reactive chlorine then engages in destructive reactions with ozone molecules. Satellite observations show a decrease of 0.4 ppbv in HCl and an increase of 0.4 ppbv in ClO inside the plume, averaged between 16 and 24 January 2022, providing direct evidence for these chlorine activation reactions. Within just one week after the volcanic eruption, stratospheric ozone partial pressure impacted by heterogeneous chemical reactions of chlorine was evidently reduced by 5% in the tropical western Pacific and Indian Ocean regions (Figure 4, Evan et al. [34]). In September–October–November 2022, the ozone loss at the midlatitudes in the Southern Hemisphere was up to −7% and the ozone concentration increased by 5% in the tropics [13]. This study only focuses on the latest two-year research after the HTHH eruption; more research associated with the ozone loss in the Antarctic polar region caused by the volcanic eruption will be published in the future.

Based on the Whole Atmosphere Community Climate Model (WACCM), it has been confirmed that the primary cause of ozone depletion in the initial eruption plume is the reaction of HOx and ClOx [24]. The crucial heterogeneous chemical reaction $HOCl + HCl \rightarrow Cl_2 + H_2O$, with a reaction rate of 10^4 cm^{-3} s^{-1}, becomes the predominant process leading to ozone depletion. Notably, this differs from the spring polar ozone depletion involving $HCl + ClONO_2$. The injection of a large amount of water vapor into the stratosphere increases the relative humidity over ice by as much as 70–100%, reducing the H_2SO_4/H_2O ratio from 70% to 35%. The volcanic plume temperature also decreases by 2–6 K, and these variations accelerate the occurrence of heterogeneous chemical reactions. Understanding these intricate and extensive connections between volcanic emissions and atmospheric chemistry is crucial for improving model simulations.

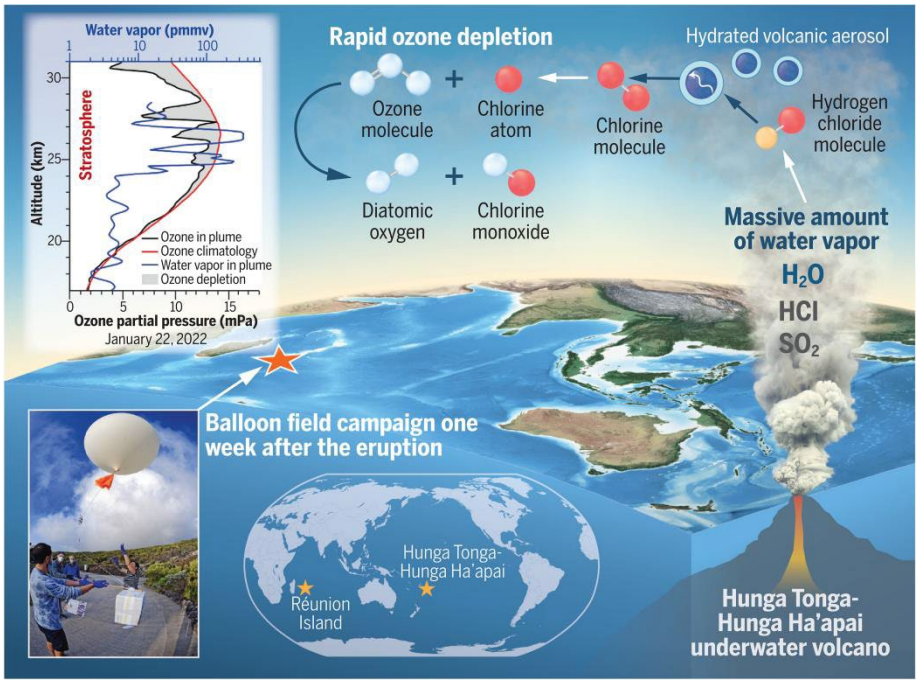

Figure 4. After the HTHH eruption, a balloon campaign took place at Reunion Island. Plume dynamics showcase the volcanic injection of H_2O vapor, sulfur dioxide (SO_2), and HCl, promoting rapid chlorine activation in hydrated volcanic aerosols and O3 depletion in the stratosphere. The 22 January 2022 O_3 profile (black line) contrasts with Reunion's climatology (red line), displaying a notable decline (from the first figure of Evan et al. [34]).

3. Discussion and Conclusions

The eruption of the HTHH volcano not only affects the atmospheric composition but also generates a series of atmospheric fluctuations with different lengths and frequencies, including surface-guided Lamb waves, acoustic waves, and gravity waves [35]. In addition to triggered wave activity, a volcano can serve as a continuous source of waves through convective plumes and latent heat release from water vapor after the initial eruption. The HTHH volcano has produced multiple atmospheric waves that propagate worldwide, with unique energy and propagation ranges [36]. Research indicates that during the initial stage of the HTHH volcanic eruption, gravity waves generated by mechanical oscillations experienced continuous amplification of amplitude during their propagation in the middle atmosphere. The amplitude and phase velocity exceeded historical records [37]. These atmospheric disturbances pose a series of challenges and risks to aircraft and spacecraft. Moreover, abnormal gravity waves may cause unexpected deviations in the trajectory of stratospheric balloons, resulting in loss of control and their drifting out of safe and controlled airspace.

In addition, large volcanic eruptions can cause ionospheric disturbances. These disturbances are mostly driven by the upward propagation of Rayleigh waves and gravity waves, and they become the primary driving force behind ionospheric disturbances. After the HTHH volcanic eruption, ionospheric disturbances (TIDs) originating from the volcanic center were detected by the global navigation satellite system, demonstrating the sensitivity of the ionosphere to atmospheric anomalies [38]. Moreover, the atmospheric waves generated by the HTHH volcanic eruption propagated throughout the Earth's upper atmosphere for several days, further causing the generation of equatorial ionospheric plasma bubbles. These plasma bubbles create irregular regions with reduced plasma density in the F-layer of the equatorial ionosphere and can seriously interfere with satellite communications [39]. Plasma bubbles are typically generated by solar activity, but intense volcanic activity can also lead to ionospheric anomalies. For stratospheric long-duration aircraft or balloons, the irregular plasma disturbances in the ionosphere can induce multipath propagation and

refraction of wireless communication signals, resulting in signal attenuation or delay. This can negatively impact satellite communications and long-endurance aerostats.

The HTHH volcanic eruption in 2022 significantly affected the stratospheric environment (e.g., water vapor, aerosols, ozone, and equipment materials). First, the HTHH volcanic eruption injected a large amount of water vapor into the stratosphere, altering the concentration and distribution of water vapor in the stratosphere and impacting stratospheric chemistry, radiation balance, and climate. The aerosol optical depth variation in the stratosphere after a volcanic eruption impacts radiative forcing. Therefore, the strengthening of stratospheric chemistry–aerosol–climate models will be useful for estimating the climate effects of volcanic eruptions [40]. Although the HTHH volcano injected only 0.2–0.5 Tg of SO_2 into the stratosphere, the SO_2 quickly transformed into sulfate aerosols due to the increased water vapor in the stratosphere. Additionally, the enhanced water vapor increased the surface area of stratospheric aerosols and induced heterogeneous chlorine chemical reactions on the surface of volcanic aerosols. This led to the depletion of stratospheric ozone during the first stage and further affected chemical reactions in the stratosphere. Finally, atmospheric waves and ionospheric disturbances triggered by the HTHH volcanic eruption may negatively impact spacecraft and aerostats.

In conclusion, due to the lack of measurements of volcanic plumes during the early stages of eruptions, there is considerable uncertainty regarding the evolution and effects of volcanic aerosols. However, studies have shown that volcanic activity impacts the stratosphere. Further research is needed to investigate the impact of atmospheric waves and ionospheric disturbances on aviation equipment materials. Increasing attention, research, and interdisciplinary cooperation will contribute to a better understanding and response to the challenges and impacts of the HTHH volcano eruption in the future.

Author Contributions: Q.S. and D.L., writing—original draft preparation; T.L. and J.X., writing—review and editing. All authors have read and agreed to the published version of the manuscript.

Funding: This work was supported by the National Natural Science Foundation of China (Grant Nos. 41975050), and a joint NSFC-DFG research project (NSFC grant no. 42061134012).

Institutional Review Board Statement: Not applicable.

Informed Consent Statement: Not applicable.

Data Availability Statement: The MLS and water vapor data were downloaded from https://acdisc.gesdisc.eosdis.nasa.gov/data/, accessed on 20 April 2022.

Conflicts of Interest: The authors declare no conflicts of interest.

References

1. Bates, S.; Carlowicz, M. Tonga Volcano Plume Reached the Mesosphere, Edited. 2022. Available online: https://earthobservatory.nasa.gov/images/149474/tonga-volcano-plume-reached-the-mesosphere (accessed on 10 April 2022).
2. Proud, S.R.; Prata, A.T.; Schmauß, S. The January 2022 eruption of Hunga Tonga-Hunga Ha'apai volcano reached the mesosphere. *Science* **2022**, *378*, 554–557. [CrossRef] [PubMed]
3. Khaykin, S.; Podglajen, A.; Ploeger, F.; Grooß, J.-U.; Tence, F.; Bekki, S.; Khlopenkov, K.; Bedka, K.; Rieger, L.; Baron, A.; et al. Global perturbation of stratospheric water and aerosol burden by Hunga eruption. *Commun. Earth Environ.* **2022**, *3*, 316. [CrossRef]
4. Carr, J.L.; Horvath, A.; Wu, D.L.; Friberg, M.D. Stereo Plume Height and Motion Retrievals for the Record-Setting Hunga Tonga-Hunga Ha'apai Eruption of 15 January 2022. *Geophys. Res. Lett.* **2022**, *49*, e2022GL098131. [CrossRef]
5. Carn, S.A.; Krotkov, N.A.; Fisher, B.L.; Li, C. Out of the blue: Volcanic SO_2 emissions during the 2021-2022 eruptions of Hunga Tonga–Hunga H'apai (Tonga). *Front. Earth Sci.* **2022**, *10*, 976962. [CrossRef]
6. Millán, L.; Santee, M.L.; Lambert, A.; Livesey, N.J.; Werner, F.; Schwartz, M.J.; Pumphrey, H.C.; Manney, G.L.; Wang, Y.; Su, H.; et al. The Hunga Tonga–Hunga Ha'apai Hydration of the Stratosphere. *Geophys. Res. Lett.* **2022**, *49*, e2022GL099381. [CrossRef]
7. Guo, S.; Bluth, G.J.S.; Rose, W.I.; Watson, I.M.; Prata, A.J. Re-evaluation of SO_2 release of the 15 June 1991 Pinatubo eruption using ultraviolet and infrared satellite sensors. *Geochem. Geophys. Geosyst.* **2004**, *5*, Q04001. [CrossRef]
8. Zhang, H.; Wang, F.; Li, J.; Duan, Y.; Zhu, C.; He, J. Potential Impact of Tonga Volcano Eruption on Global Mean Surface Air Temperature. *J. Meteorol. Res.* **2022**, *36*, 1–5. [CrossRef]

9. Zuo, M.; Zhou, T.; Man, W.; Chen, X.; Liu, J.; Liu, F.; Gao, C. Volcanoes and Climate: Sizing up the Impact of the Recent Hunga Tonga-Hunga Ha'apai Volcanic Eruption from a Historical Perspective. *Adv. Atmos. Sci.* **2022**, *39*, 1986–1993. [CrossRef]
10. Duchamp, C.; Wrana, F.; Legras, B.; Sellitto, P.; Belhadji, R.; von Savigny, C. Observation of the aerosol plume from the 2022 Hunga Tonga—Hunga Ha'apai eruption with SAGE III/ISS. *Geophys. Res. Lett.* **2023**, *50*, e2023GL105076. [CrossRef]
11. Boichu, M.; Grandin, R.; Blarel, L.; Torres, B.; Derimian, Y.; Goloub, P.; Brogniez, C.; Chiapello, I.; Dubovik, O.; Mathurin, T.; et al. Growth and global persistence of stratospheric sulfate aerosols from the 2022 Hunga Tonga–Hunga Ha'apai volcanic eruption. *J. Geophys. Res. Atmos.* **2023**, *128*, e2023JD039010. [CrossRef]
12. Zhu, Y.; Portmann, R.W.; Kinnison, D.; Toon, O.B.; Millán, L.; Zhang, J.; Vömel, H.; Tilmes, S.; Bardeen, C.G.; Wang, X.; et al. Stratospheric ozone depletion inside the volcanic plume shortly after the 2022 Hunga Tonga eruption. *Atmos. Chem. Phys.* **2023**, *23*, 13355–13367. [CrossRef]
13. Sellitto, P.; Podglajen, A.; Belhadji, R.; Boichu, M.; Carboni, E.; Cuesta, J.; Duchamp, C.; Kloss, C.; Siddans, R.; Bègue, N.; et al. The unexpected radiative impact of the Hunga Tonga eruption of 15th January 2022. *Commun. Earth Environ.* **2022**, *3*, 288. [CrossRef]
14. Jenkins, S.; Smith, C.; Allen, M.; Grainger, R. Tonga eruption increases chance of temporary surface temperature anomaly above 1.5 °C. *Nat. Clim. Change* **2023**, *13*, 127–129. [CrossRef]
15. Wilmouth, D.M.; Østerstrøm, F.F.; Smith, J.B.; Anderson, J.G.; Salawitch, R.J. Impact of the Hunga Tonga volcanic eruption on stratospheric composition. *Proc. Natl. Acad. Sci. USA* **2023**, *120*, e2301994120. [CrossRef] [PubMed]
16. Vömel, H.; Evan, S.; Tully, M. Water vapor injection into the stratosphere by Hunga Tonga–Hunga Ha'apai. *Science* **2022**, *377*, 1444–1447. [CrossRef]
17. Randel, W.J.; Johnston, B.R.; Braun, J.J.; Sokolovskiy, S.; Vömel, H.; Podglajen, A.; Legras, B. Stratospheric Water Vapor from the Hunga Tonga-Hunga H'apai Volcanic Eruption Deduced from COSMIC-2 Radio Occultation. *Remote Sens.* **2023**, *15*, 2167. [CrossRef]
18. Bian, J.; Li, D.; Bai, Z.; Xu, J.; Li, Q.; Wang, H.; Vömel, H.; Wienhold, F.; Thomas, P. First detection of aerosols of the Hunga Tonga eruption in the Northern Hemisphere stratospheric westerlies. *Sci. Bull.* **2023**, *68*, 574. [CrossRef]
19. Xu, J.; Li, D.; Bai, Z.; Tao, M.; Bian, J. Large amounts of water vapor were injected into the stratosphere by the Hunga Tonga–Hunga Ha'apai volcano eruption. *Atmosphere* **2022**, *13*, 912. [CrossRef]
20. Schoeberl, M.R.; Wang, Y.; Ueyama, R.; Taha, G.; Jensen, E.; Yu, W. Analysis and Impact of the Hunga Tonga–Hunga Ha'apai Stratospheric Water Vapor Plume. *Geophys. Res. Lett.* **2022**, *49*, e2022GL100248. [CrossRef]
21. Coy, L.; Newman, P.A.; Wargan, K.; Partyka, G.; Strahan, S.E.; Pawson, S. Stratospheric Circulation Changes Associated With the Hunga Tonga–Hunga Ha'apai Eruption. *Geophys. Res. Lett.* **2022**, *49*, e2022GL100982. [CrossRef]
22. Taha, G.; Loughman, R.; Colarco, P.R.; Zhu, T.; Thomason, L.W.; Jaross, G. Tracking the 2022 Hunga Tonga–Hunga Ha'apai Aerosol Cloud in the Upper and Middle Stratosphere Using Space–Based Observations. *Geophys. Res. Lett.* **2022**, *49*, e2022GL100091. [CrossRef] [PubMed]
23. Legras, B.; Duchamp, C.; Sellitto, P.; Podglajen, A.; Carboni, E.; Siddans, R.; Grooß, J.-U.; Khaykin, S.; Ploeger, F. The evolution and dynamics of the Hunga Tonga–Hunga Ha'apai sulfate aerosol plume in the stratosphere. *Atmos. Chem. Phys.* **2022**, *22*, 14957–14970. [CrossRef]
24. Zhu, Y.; Bardeen, C.G.; Tilmes, S.; Mills, M.J.; Wang, X.; Harvey, V.L.; Taha, G.; Kinnison, D.; Portmann, R.W.; Yu, P.; et al. Perturbations in stratospheric aerosol evolution due to the water-rich plume of the 2022 Hunga–Tonga eruption. *Commun. Earth Environ.* **2022**, *3*, 248. [CrossRef]
25. Asher, E.; Todt, M.; Rosenlof, K.; Thornberry, T.; Gao, R.S.; Taha, G.; Walter, P.; Alvarez, S.; Flynn, J.; Davis, S.M.; et al. Unexpectedly rapid aerosol formation in the Hunga Tonga plume. *Proc. Natl. Acad. Sci. USA* **2023**, *120*, e2219547120. [CrossRef] [PubMed]
26. Kloss, C.; Sellitto, P.; Renard, J.; Baron, A.; Bègue, N.; Legras, B.; Berthet, G.; Briaud, E.; Carboni, E.; Duchamp, C.; et al. Aerosol Characterization of the Stratospheric Plume From the Volcanic Eruption at Hunga Tonga 15 January 2022. *Geophys. Res. Lett.* **2022**, *49*, e2022GL099394. [CrossRef]
27. Deshler, T.; Johnson, B.J.; Rozier, W.R. Balloonborne measurements of Pinatubo aerosol during 1991 and 1992 at 41°N: Vertical profiles, size distribution, and volatility. *Geophys. Res. Lett.* **1993**, *20*, 1435–1438. [CrossRef]
28. Yuen, D.A.; Scruggs, M.A.; Spera, F.J.; Zheng, Y.; Hu, H.; McNutt, S.R.; Thompson, G.; Mandli, K.; Keller, B.R.; Wei, S.S.; et al. Under the surface: Pressure-induced planetary-scale waves, volcanic lightning, and gaseous clouds caused by the submarine eruption of Hunga Tonga-Hunga Ha'apai volcano. *Earthq. Res. Adv.* **2022**, *2*, 100134. [CrossRef]
29. Bian, J.; Pan, L.L.; Paulik, L.; Vömel, H.; Chen, H.; Lu, D. In situ water vapor and ozone measurements in Lhasa and Kunming during the Asian summer monsoon. *Geophys. Res. Lett.* **2012**, *39*, L19808. [CrossRef]
30. Li, D.; Vogel, B.; Bian, J.; Müller, R.; Pan, L.L.; Günther, G.; Bai, Z.; Li, Q.; Zhang, J.; Fan, Q.; et al. Impact of typhoons on the composition of the upper troposphere within the Asian summer monsoon anticyclone: The SWOP campaign in Lhasa 2013. *Atmos. Chem. Phys.* **2017**, *17*, 4657–4672. [CrossRef]
31. Ma, D.; Bian, J.; Li, D.; Bai, Z.; Li, Q.; Zhang, J.; Wang, H.; Zheng, X.; Hurst, D.; Vömel, H. Mixing characteristics within the tropopause transition layer over the Asian summer monsoon region based on ozone and water vapor sounding data. *Atmos. Res.* **2022**, *271*, 106093. [CrossRef]
32. Yang, Z.; Li, D.; Luo, J.; Tian, W.; Bai, Z.; Li, Q.; Zhang, J.; Wang, H.; Zheng, X.; Vömel, H.; et al. Determination of cirrus occurrence and distribution characteristics over the Tibetan Plateau based on the SWOP campaign. *J. Geophys. Res. Atmos.* **2023**, *128*, e2022JD037682. [CrossRef]

33. Santee, M.L.; Lambert, A.; Froidevaux, L.; Manney, G.L.; Schwartz, M.J.; Millán, L.F.; Livesey, N.J.; Read, W.G.; Werner, F.; Fuller, R.A. Strong Evidence of Heterogeneous Processing on Stratospheric Sulfate Aerosol in the Extrapolar Southern Hemisphere Following the 2022 Hunga Tonga–Hunga Ha'apai Eruption. *J. Geophys. Res. Atmos.* **2023**, *128*, e2023JD039169. [CrossRef]
34. Evan, S.; Brioude, J.; Rosenlof, K.H.; Gao, R.S.; Portmann, R.W.; Zhu, Y.; Volkamer, R.; Lee, C.F.; Metzger, J.M.; Lamy, K.; et al. Rapid ozone depletion after humidification of the stratosphere by the Hunga Tonga Eruption. *Science* **2023**, *382*, 6668. [CrossRef] [PubMed]
35. Matoza, R.S.; Fee, D.; Assink, J.D.; Iezzi, A.M.; Green, D.N.; Kim, K.; Toney, L.; Lecocq, T.; Krishnamoorthy, S.; Lalande, J.M.; et al. Atmospheric waves and global seismoacoustic observations of the January 2022 Hunga eruption, Tonga. *Science* **2022**, *377*, 95–100. [CrossRef] [PubMed]
36. Wright, C.J.; Hindley, N.P.; Alexander, M.J.; Barlow, M.; Hoffmann, L.; Mitchell, C.N.; Prata, F.; Bouillon, M.; Carstens, J.; Clerbaux, C.; et al. Surface-to-space atmospheric waves from Hunga Tonga–Hunga Ha'apai eruption. *Nature* **2022**, *609*, 741–746. [CrossRef]
37. Wu, H.; Lu, X.; Wang, W.; Liu, H.L. Simulation of the Propagation and Effects of Gravity Waves Generated by Tonga Volcano Eruption in the Thermosphere and Ionosphere Using Nested–Grid TIEGCM. *J. Geophys. Res. Space Phys.* **2023**, *128*, e2023JA031354. [CrossRef]
38. Salikhov, N.; Shepetov, A.; Pak, G.; Saveliev, V.; Nurakynov, S.; Ryabov, V.; Zhukov, V. Disturbances of Doppler Frequency Shift of Ionospheric Signal and of Telluric Current Caused by Atmospheric Waves from Explosive Eruption of Hunga Tonga Volcano on January 15, 2022. *Atmosphere* **2023**, *14*, 245. [CrossRef]
39. Shinbori, A.; Sori, T.; Otsuka, Y.; Nishioka, M.; Perwitasari, S.; Tsuda, T.; Kumamoto, A.; Tsuchiya, F.; Matsuda, S.; Kasahara, Y.; et al. Generation of equatorial plasma bubble after the 2022 Tonga volcanic eruption. *Sci. Rep.* **2023**, *13*, 6450. [CrossRef] [PubMed]
40. Zhou, T.; Zuo, M.; Man, W. Recent advances and future avenues in examining the impacts of volcanic aerosols on climate. *Chin. Sci. Bull.* **2024**, *69*, 230–252. [CrossRef]